Monolithic High-Tc Superconducting Phase Shifter at 10 GHz

June H. Takemoto-Kobayashi, Charles M. Jackson, Emery B. Guillory, Claire Pettiette-Hall, John F. Burch

TRW, Space and Technology Group, One Space Park, Redondo Beach, CA 90278

Abstract

We describe a monolithic high temperature superconductor (HTS) phase shifter integrated into a 10 GHz microstrip line. This is the first demonstration of a non-resonant HTS circuit based on our design. We observed phase shifts greater than 150 degrees in resonant structures, and 20 degrees in broadband circuits.

Introduction

High temperature superconductivity (HTS) can provide high quality films for passive microwave devices [1, 2], but nonlinear superconducting Josephson elements for active circuits have been difficult to fabricate. Progress in HTS technology enables the fabrication and test of a new broadband HTS phase shifter which employs a high density of superconductive quantum interference devices (SQUIDs). This paper describes the performance of a broadband HTS phase shifter operating at 10 GHz.

Phase shifters are key elements for phased array antennas. A number of uniquely superconducting approaches have been attempted to provide phase control at microwave frequencies [3]. Superconducting phase shift mechanisms include varying the kinetic inductance of thin superconducting films [4], the use of a novel transistor analogy [5], and cascading a series array of Josephson junctions [6].

The distributed Josephson inductance (DJI) approach [7]consists of a superconducting transmission line that is actively coupled to an array of SQUIDs distributed along its length as shown in Figure 1. Each SQUID consists of a single HTS microbridge Josephson element shunted by the inductance of the hole in the microstrip line. The Josephson inductance from the SQUIDs provides a variable inductance along the line. By applying flux to the SQUIDs, either through a control current along the transmission line or by an external magnetic field, the inductance distributed along the transmission line can be controlled. The inductance controls the wave velocity, and hence phase delay of the transmission line. The advantage of the DJI phase shifter is that it provides phase shift with low loss and scalability to higher frequencies providing a true time delay.

We have succeeded in a series of DJI phase shifter demonstrations. Earlier versions of the DJI phase shifter were successfully fabricated and tested in low temperature Nb technology [7]. Later, when HTS SQUIDs became available, a single SQUID was specially selected and coupled to a microstrip resonator [8]. As the maturity of HTS microbridges increased, a total of 40 SQUIDs were monolithically integrated into a single microstrip resonator [9]. The maturity of HTS processing continues to improve, and it is now possible to fabricate and test a broadband non-resonant HTS phase shifter with greater than 2000 microbridges per wavelength at 10 GHz monolithically integrated into the active region of the phase shifter.

Fabrication

The new HTS phase shifter requires fabrication of a large array of step-edge HTS SQUIDs [10]. We pattern HTS microbridges over sharp steps etched in the 20-mil thick $LaAlO_3$ substrate. A steep 0.3 μm edge is ion-milled into the substrate, and an HTS film (0.2 μm) is deposited over the entire area. The film is then patterned and ion-milled to produce a 2-μm wide microbridge over the step-edge, resulting in an engineered weak link Josephson element.

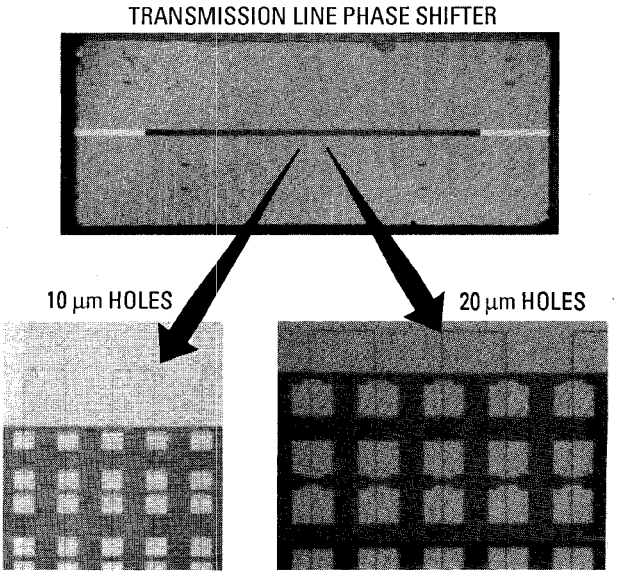

Figure 1. Photo of HTS phase shifter. Dark areas are the YBCO HTS material and the faint rectangular outlines are the steps in the $LaAlO_3$ substrate. Square holes are cut out of the HTS adjacent to 2μm microbridges.

Figure 1 shows a photo of the fabricated HTS SQUIDs on the microstrip phase shifters. In the detailed blow up of the active region, the 2-μm step-edge microbridge and the pair of inductive square holes (10 or 20 μm) make up a single rf SQUID. These SQUIDs are duplicated in parallel as a column across the width of the microstrip. These columns of SQUIDs are in turn laid out in series along the length of the resonator or transmission line.

Design and Theory of Operation

The most important properties of the DJI are the response to a control field and the magnitude of the phase shift. This section finds the current per flux quantum Iϕ and the change in inductance normalized to the total inductance per unit length ΔL/L (which is related to the phase shift). The HTS DJI uses a planar geometry with square holes (of side a) spaced a distance d apart, filling the microstrip line (of width w) over a ground plane a distance h below (Figure 2).

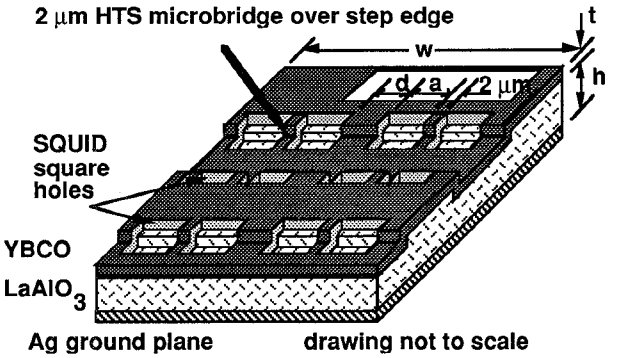

Figure 2. Perspective drawing of SQUID geometry. HTS (YBCO) of thickness t (0.3 μm) is deposited on top of a 20-mil (height h) $LaAlO_3$ substrate with 0.6 μm of Ag ground plane. SQUID holes are squares of side a with spacing d apart on a microstrip of width w. Hole pairs are joined by a 2 μm HTS microbridge weak link that steps over a 0.3 μm $LaAlO_3$ step.

The change in inductance for a single pair of loops (with a single junction) is determined in two limits. The first limit, a low coupling limit, uses Ampere's law to find the magnetic field and mutual inductance, and the other uses a high coupling limit where the mutual inductance is taken as the loop inductance. Both limits assume that the current is uniform over the microstrip line; a limit that is most valid for wide lines. The current per flux quantum Φ_0 can be measured to determine which model is the better estimate. For the low coupling limit,

$$I_\Phi = \frac{2\pi d W \Phi_o}{3\mu_o a^3} \quad (1)$$

and for the high coupling limit

$$I_\Phi = \frac{4W\Phi_o}{15\mu_o a^2} \quad (2)$$

Using these expressions, the expression for the mutual inductance, and the definition of the coupling constant k,

$$k^2 = \frac{M^2}{L_{sq}L_{ms}} \quad (3)$$

SQUID loop inductance Lsq,

$$L_{sq} = 1.25\mu_o a \quad (4)$$

and the microstrip inductance Lms (for a length a):

$$L_{ms} = \frac{\mu_o h a}{W} \quad (5)$$

We find the total changes in inductance from [7 ,11]

$$\frac{\Delta L_{one}}{L_{one}} = k^2\beta \quad (6)$$

provided we have satisfied the inequality

$$\beta = \frac{2\pi L_{sq} I_c}{\Phi_o} < 1 \quad (7)$$

The microbridge critical current Ic is typically between 100 μA (at 4 K) and 30 μA (at 65 K) for 2 μm HTS step edge microbridges. The condition (ß=1) obtains the maximum change in inductance and sets the size of the loops. Combining these terms, we obtain a value for low coupling Ampere's loop calculation:

$$\frac{\Delta L_T}{L_T} = \frac{6a^4\beta}{5\pi^2 d^2 h(a+d)} \quad (8)$$

and for high coupling limit:

$$\frac{\Delta L_T}{L_T} = \frac{15a^2\beta}{2h(a+d)} \quad (9)$$

The high coupling limit is about 60 times larger than the Ampere's loop limit. Note that these two expressions do not depend on the width explicitly, but they do depend on the loop size a, spacing d, and substrate height h. In the limit of a=d the change in inductance is proportional to a/h for both the Ampere's loop and high coupling limit calculation. For maximum phase shift, the hole size a should be as large as possible, and h should be as small as possible.

The experimental results, provided in the Table I, show that the high coupling limit provides the best estimate on the performance of the devices.

SQUID size	10 μm Hole		20 μm Hole	
Coupling Limit	Low	High	Low	High
Lsq	16 pH		32 pH	
ß (Ic=100 μA)	5		10	
Iϕ (Theory)	4.3 mA	1.1 mA	0.54 mA	0.27 mA
Iϕ (Exp)	1.0 mA		0.39 mA	
Δvp/vp	0.0006	0.037	0.0064	0.098
ΔΦ (Theory)	0.11°	6.6°	1.15°	17.6°
ΔΦ (Exp)	8°		20°	

Table I. Summary of calculated and measured parameters of phase shifters in a broadband circuit at 10 GHz

Measurements and Results

A phase change of over 190 degrees was measured for the resonant phase shifter using the external coil method. Figure 3 plots the phase as a function of coil current at 4 K. Measurable phase shifts were detected up to 65 K. Input power was typically set to -40 dBm.

Figure 4 shows the power dependence of the resonating phase shifter for the new high SQUID density phase shifter as compared to the results reported previously [9]. The newer devices have improved their power handling from -50 dBm to over -10 dBm, while the phase shift has increased from 50 degrees to over 190 degrees. Notice that a phase shift over 180 degrees was achieved due the change in phase velocity caused by kinetic inductance effects of the superconducting microstrip.

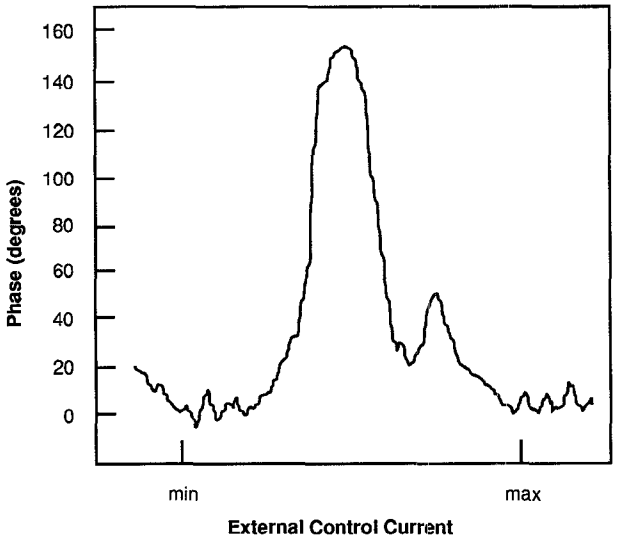

Figure 3. Phase as a function of external field for resonant phase shifter at 10 GHz at 4 K and -40 dBm input power.

Phase change was measured with a modulated magnetic field using either current through external coil or a direct current passed down the transmissionline for the straight transmission line phase shifters. When the external coil provided the varying magnetic field, the transmission line circuit shifted phase by 13 degrees at -30 dBm input power. Figures 5 plots the temperature dependence of the phase shift using this method for a straight through circuit. The insertion loss is shown on Figure 6 as a function of temperature at -20 dB power.

When direct current is passed down the transmission line through the SQUIDs, the circuits yield a phase shift of 20 degrees as shown in Figure 7. The periodicity of the phase shift using internal control current is 240 μA at 10 K to 14 μA at 67 K. Phase begins shifting significantly near the critical current of HTS circuit which is typically around 100 - 300 μA. As shown in Figure 1, the circuit layout we are using has a step edge all the way across the microstrip, so an alternate circuit model is a series of parallel array of junctions.

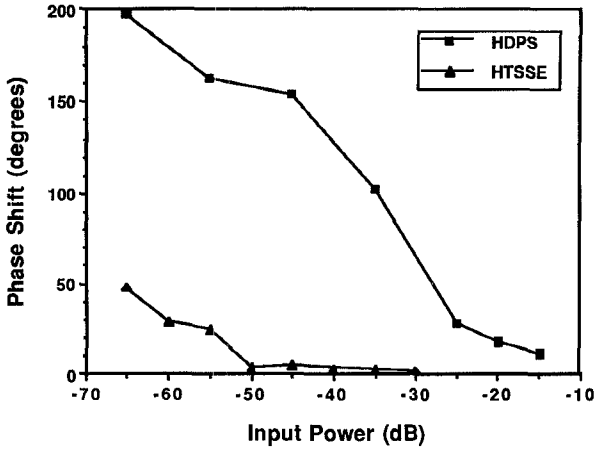

Figure 4. Plot of peak to peak phase shift versus input power for a resonator with 10-μm hole SQUIDs shows significant improvement in power and phase shift of this work on over a previously reported HTS phase shifter [6].

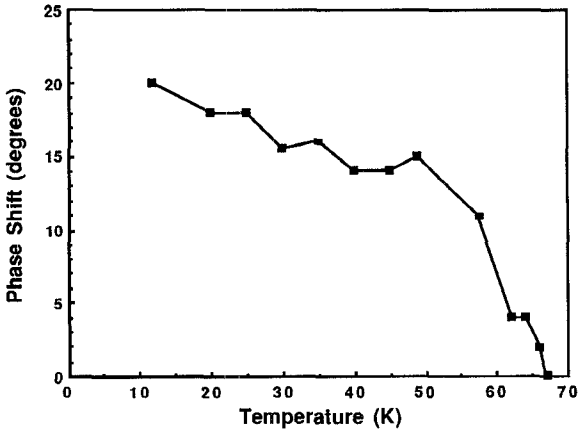

Figure 5. Temperature dependence of non-resonant 20-μm hole SQUID phase shifter was measured using external field control through transmission line at -30 dBm input power and 9.4 GHz. Phase shift is maintained near 15 degrees from 4.2 K to 50 K. Detectable phase shifts were measured up to 67 K.

The series junctions mask the coupling of the control current and limit the maximum current to a value below Iϕ. This dependence on Ic appears to concur with a series array of Josephson junctions analyzed by G. Chen [6]. We have compensated this series array effect in a new mask for future studies of HTS phase shifters by changing the step-edge area, and also by improving the HTS deposition process to prevent weak links from forming outside of the SQUIDs.

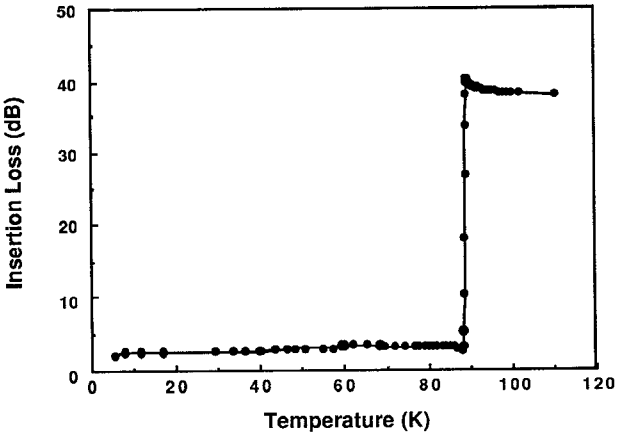

Figure 6. Insertion loss of a nonresonant phase shifter with 20 μm SQUIDs. Input power of -20 dBm was applied to the circuit.

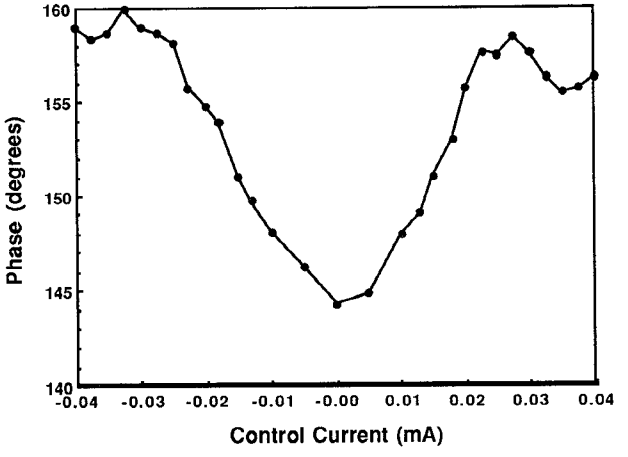

Figure 7. This plot shows phase shift versus control current where direct current was passed along the straight through transmission line containing the 20-μm hole SQUIDs. Phase was measured at a temperature of 44K and an input power of -40 dBm.

Conclusion

We have presented data on an HTS monolithic phase shifter using over two thousand integrated SQUID devices per wavelength. Phase shifts of 20 degrees were observed in transmission line circuits, and phase shifts of greater than 190 degrees were observed in the resonant circuits. The high coupling limit is the best model for the circuit. This high temperature superconducting phase shifter is suitable for integration into phased array antenna systems for communications applications.

Acknowledgements

This research was funded under the SDIO Materials and Structures Program through ONR contract N00014-91-C-0200. The authors would like to thank Kevin W. Kobayashi for his technical advice on microwave propagation, Andrew Smith for his comments and suggestions, Dale Durand for his technical advice in the theory of SQUIDs, Aron Kain for the circuit layout, Chuong Dang for sawing and ribbon bonding of chips, and Alfred Lee for discussions about the deposition process.

References

1 J. H. Takemoto, C. M. Jackson, R. Hu, J. F. Burch, K. P. Daly, and R. W. Simon, "Microstrip Resonators and Filters Using High-Tc Superconducting Thin Films on $LaAlO_3$ ", *IEEE Transactions on Magnetics*, vol. MAG-27, pp. 2549-2552, March 1991.

2 J. H. Takemoto, C. M. Jackson, H. M. Manasevit, D. C. St. John, J. F. Burch, K. P. Daly, and R. W. Simon, "Microstrip resonators using two-sided metalorganic chemical vapor deposited Er-Ba-Cu-O thin films," Applied Physics Letters, vol 58, no. 10, pp. 1109-1111, 11 March 1991.

3 R. C. Hansen, "Antenna Applications of Superconductivity", *IEEE Transactions on Microwave Theory and Techniques,* MTT-39, no. 9, pp. 1508-1512, Sept. 1991.

4 J. M. Pond, J. H. Claassen, W. L. Carter, "Measurements and Modeling of Kinetic Inductance Microstrip Delay Lines," *IEEE Transactions on Microwave Theory and Techniques*, MTT-35, no. 12, pp. 1256-1262, Dec. 1987.

5 J. Martens, to be published in *IEEE Transactions on Microwave Theory and Techniques*, Dec. 1991.

6 G. Chen, "Shock-wave Generation and Pulse Sharpening on a Series Array Josephson Function Transmission Line," *IEEE Trans. on Applied Superconductivity*, vol. 1, no. 3, pp. 140-144, Sept. 1991.

7 D. J. Durand, J. Carpenter, E. Ladizinsky, L. Lee, C. Jackson, A. H. Silver, and A. D. Smith, "The Distributed Josephson Inductance Phase Shifter," to be published in *IEEE Trans. Applied Superconductivity*, March 1992..

8 C. M. Jackson, and D. J. Durand, "10 GHz High Temperature Superconductor Phase Shifter", presented at the 1991 IEEE MTT-S Symposium, June 1991.

9 J. H. Takemoto-Kobayashi, C. M. Jackson, C. Pettiette-Hall, J. F. Burch, "High-Tc Superconductor Monolithic Phase Shifter," to be published in *IEEE Trans. on Applied Superconductivity*, March 1992.

10 K. P. Daly, J. Burch, S. Coons, R. Hu, "YBa2Cu3O7 Step-edge RF SQUID Biased at 10 GHz," IEEE Transactions on Magnetics, MAG-27, pp. 3066-3069, March 1991.

11 A. Barone and G. Paterno, Physics and Applications of the Josephson Effect, New York: Wiley-Interscience Publications, 1982, pp. 384.